Bruurs et al., http://www.jcb.org/cgi/content/full/jcb.201505118/DC1

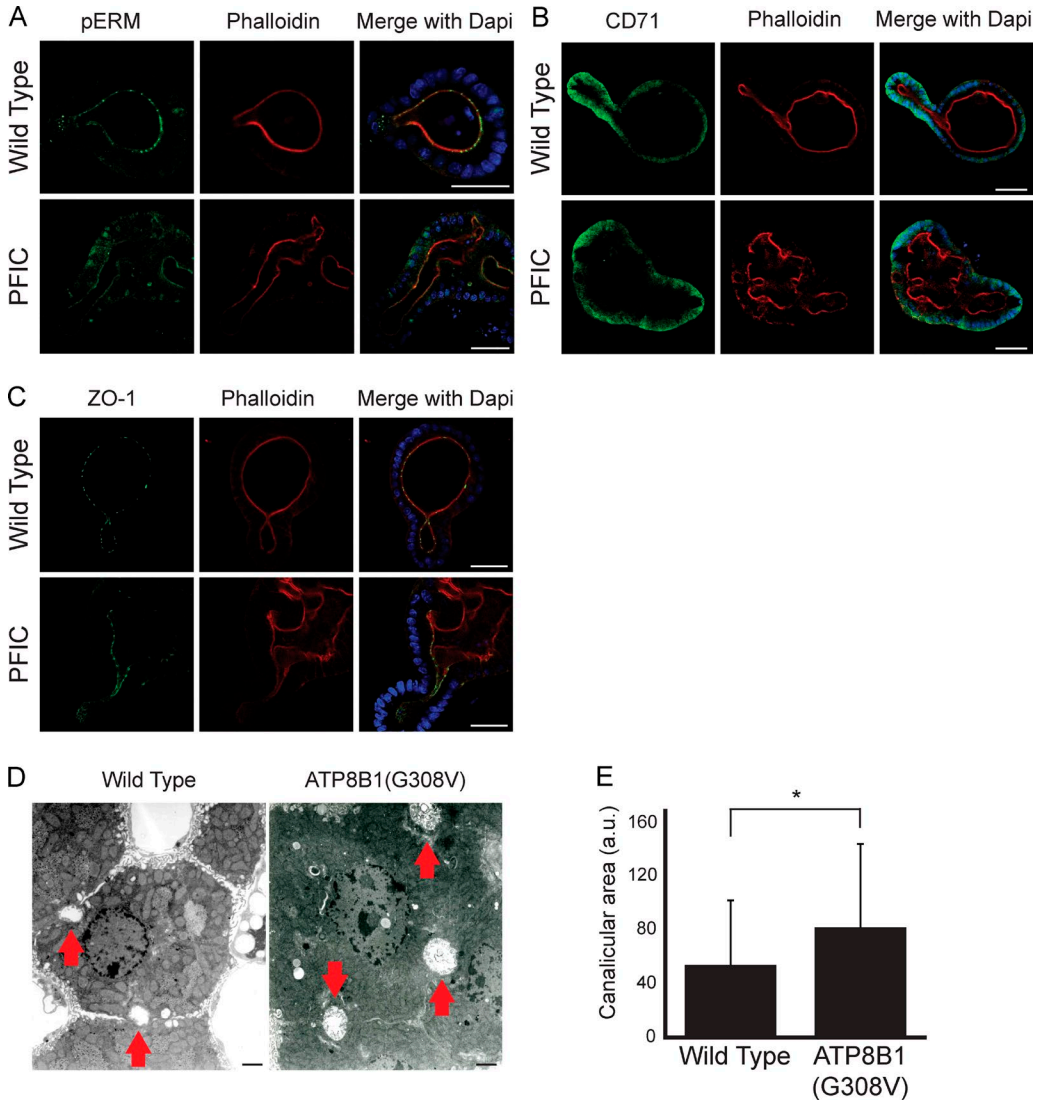

Figure S1. **ATP8B1 mutations affect lumen morphology in the intestine and liver.** (A–C) Localization of the apical marker pERM (A), basolateral marker CD71 (B), and apical tight junction marker ZO-1 (C) in WT and PFIC organoids. (D) Transmission electron micrographs of liver sections from WT or *ATP8B1*$^{G308V/G308V}$ mice. Red arrows highlight bile canaliculi. (E) Quantification of bile canalicular lumen size in WT or *ATP8B1*$^{G308V/G308V}$ mice. WT n = 138, *ATP8B1*$^{G308V/G308V}$ n = 146 (total number of canaliculi from two different mice per genotype). Error bars are SD. *, $P < 0.00003$. Bars: (A–C) 35 µm; (D) 500 nm.

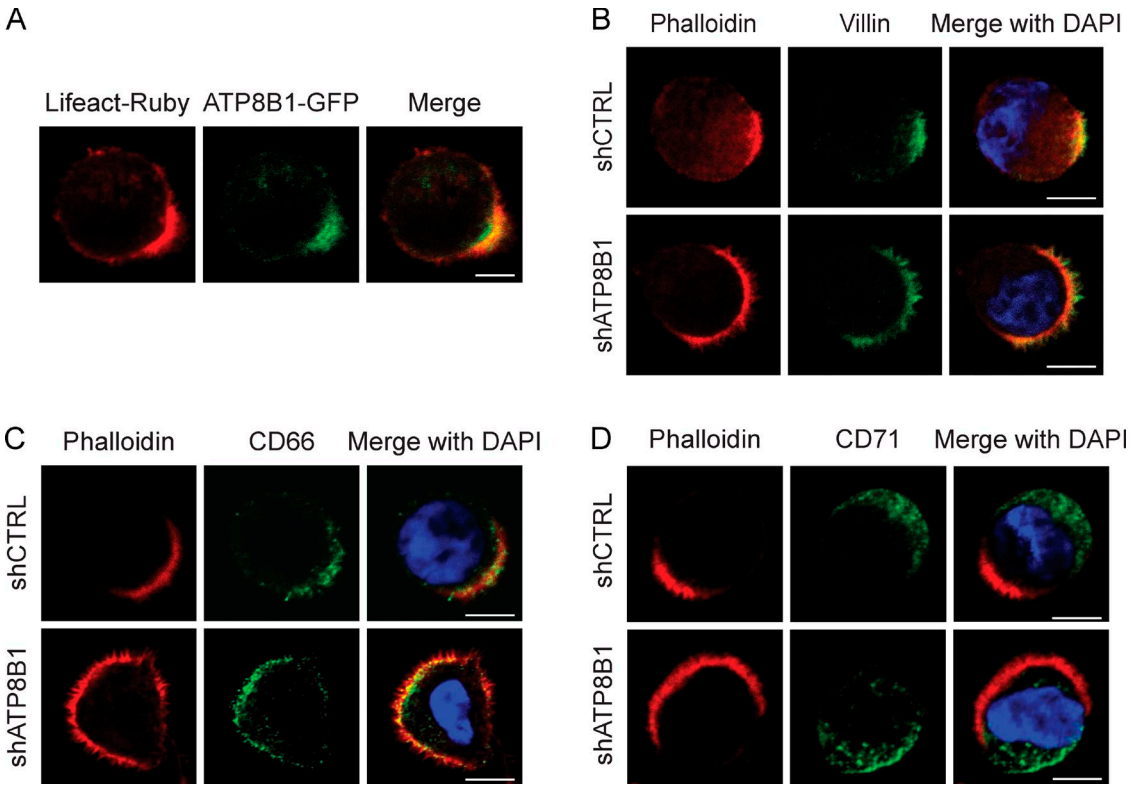

Figure S2. **Polarity markers distribute normally in ATP8B1-depleted W4 cells.** (A) W4 cell expressing ATP8B1-GFP and the actin marker Lifeact-Ruby. (B) Control or ATP8B1-depleted W4 cells immunostained for the brush border marker villin. (C and D) Immunofluorescence staining in polarized control or ATP8B1-depleted W4 cells demonstrates normal segregation of apical and basolateral markers (CD66 [C] and CD71 [D], respectively). Bars, 5 µm.

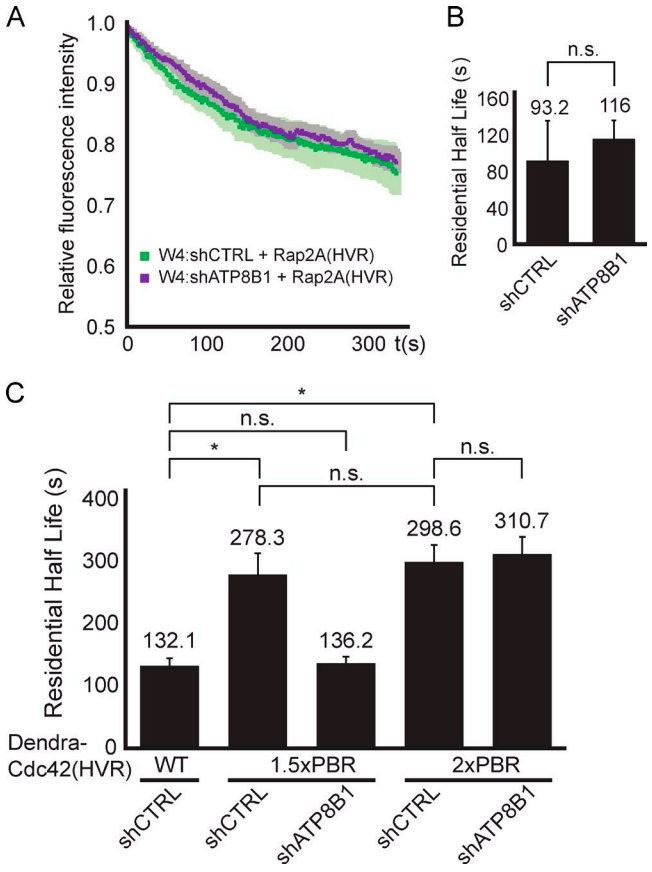

Figure S3. **ATP8B1 knockdown does not affect apical membrane diffusion of Dendra-Rap2A(HVR).** (A) Mean normalized dissociation traces for control (*n* = 9) or ATP8B1-depleted (*n* = 9) W4 cells expressing Dendra-Rap2A(HVR). Light areas indicate SEM. (B) Residential half-lives determined from mean decay traces shown in A using curve fitting. Statistics were performed using the half-lives from individual cell traces. Error bars represent SEM. n.s., $P > 0.05$. (C) Residential half-lives determined from mean decay traces shown in Fig. 5 E using curve fitting. Statistics were performed using the half-lives from individual cell traces. Error bars represent SEM. *, $P < 0.02$; n.s., $P > 0.05$.